ORIGINAL ARTICLE   **Open Access**

Development of a Wearable Upper Limb Rehabilitation Robot Based on Reinforced Soft Pneumatic Actuators

Xinbo Chen[1], Shuai Zhang[1], Kaibin Cao[1], Chunjie Wei[1], Wumian Zhao[1] and Jiantao Yao[1,2]*

Abstract

Dyskinesia of the upper limbs caused by stroke, sports injury, or traffic accidents limits the ability to perform the activities of daily living. Besides the necessary medical treatment, correct and scientific rehabilitation training for the injured joint is an important auxiliary means during the treatment of the effected upper limb. Conventional upper-limb rehabilitation robots have some disadvantages, such as a complex structure, poor compliance, high cost, and poor portability. In this study, a novel soft wearable upper limb rehabilitation robot (SWULRR) with reinforced soft pneumatic actuators (RSPAs) that can withstand high pressure and featuring excellent loading characteristics was developed. Driven by RSPAs, this portable SWULRR can perform rehabilitation training of the wrist and elbow joints. In this study, the kinematics of an SWULRR were analyzed, and the force and motion characteristics of RSPA were studied experimentally. The results provide a reference for the development and application of wearable upper limb rehabilitation robots. An experimental study on the rotation angle of the wrist and the pressure of the RSPA was conducted to test the effect of the rehabilitation training and verify the rationality of the theoretical model. The process of wrist rehabilitation training was tested and evaluated, indicating that SWULRR with RSPAs will enhance the flexibility, comfort, and safety of rehabilitation training. This work is expected to promote the development of wearable upper-limb rehabilitation robots based on modular reinforced soft pneumatic actuators.

Keywords: Upper limb rehabilitation, Reinforced soft pneumatic actuator, Wearable rehabilitation robot, Motion analysis

1 Introduction

In order to recover the motor function of each joint of the effected upper limb as soon as possible, correct and scientific assistant rehabilitation training for each joint is a necessary auxiliary method in addition to traditional medical treatment [1–3]. Rehabilitation training of upper limb joints with sports disorders can be carried out by a rehabilitation robot to prevent muscle atrophy [4–7].

Conventional rehabilitation robots mostly adopt a rigid exoskeleton structure driven by motors, which can help

the upper limbs achieve success at rehabilitation training [8]. Rigid rehabilitation robots can provide support and protection for patient arms and have the advantage of precise motion control [9]. However, the poor flexibility of a rigid exoskeleton structure may result in secondary damage to the joints owing to the impact force caused by the rapid movements of the rigid structure or inappropriate control [10, 11]. During training, the orthoses at the end of the rehabilitation robot need to be fixed onto the upper limb of the patient [12, 13], but the rigid exoskeleton structure is difficult to match up with human joints precisely. This limits the movement range of the human body and normally causes discomfort to the patient [14]. In addition, conventional rehabilitation training systems are expensive, and their structure is complex, heavy and

*Correspondence: jtyao@ysu.edu.cn

[1] Parallel Robot and Mechatronic System Laboratory of Hebei Province, Yanshan University, Qinhuangdao 066004, China
Full list of author information is available at the end of the article

non-portable, which means that rehabilitation training can only be carried out in a fixed place, and not wherever the medical needs of patients require it [15, 16].

To improve the performance of conventional rigid rehabilitation robots, many researchers have attempted to add flexible components to rehabilitation robots. Xu et al. [17–19] applied cable-driven technology in rehabilitation training. With the recent rapid development of soft materials, soft actuators have been gradually applied in the field of robot-aided rehabilitation, such as pneumatic artificial muscles [20–22], shape memory alloys [23, 24], and various polymer bladders [25, 26], which can overcome the disadvantages of conventional rigid rehabilitation robots [27, 28]. Li et al. [29] designed a soft bionic exoskeleton robot with seven degrees of freedom, driven by tendons, to assist stroke patients. Andrikopoulos et al. [30] designed a wrist exoskeleton rehabilitation robot driven by pneumatic tendons, which can make the wrist move with two degrees of freedom by controlling the length of the four pneumatic tendons. Oguntosin et al. [31] proposed an upper limb rehabilitation robot based on a polyethylene soft actuator module that can realize rehabilitation training of the elbow and shoulder joints by an expansion of each actuator module. O'Neil et al. [32] designed a wearable soft shoulder rehabilitation robot that can realize rehabilitation training for shoulder joints using two types of flexible woven fabric pneumatic actuators. Rehabilitation robots driven by soft actuators can avoid secondary injury to patients caused by improper operations or sudden accidents, advantages on which their high human-robot interaction security and excellent application prospect is based [33–36].

The main contribution of this study stems from the development and experimental evaluation of a novel wearable rehabilitation robot actuated by reinforced soft pneumatic actuators (RSPAs) that can provide a sufficient driving force for rehabilitation. The new RSPA is composed of a thermoplastic polyurethane (TPU) composite bladder and an elastic holder. The surface of the TPU composite bladder is laminated with a layer of high-strength nylon material to form a reinforced bladder structure that can withstand higher pressures while maintaining flexibility compared with a conventional bladder. These new soft actuators were applied to a wearable soft exoskeleton robot for human upper limb rehabilitation. This portable wearable rehabilitation robot can perform rehabilitation training of the wrist and elbow joints through the expansion and deformation of RSPAs.

The wearable rehabilitation robot designed in this study features the following: (a) it can carry out rehabilitation training for wrist and elbow joints according to the needs of the patients; (b) it is composed of soft components, which endows the device with high human-robot

interaction security; (c) the robot itself and its maintenance cost very little; (d) it can carry out rehabilitation training anytime and anywhere according to the needs of patients, which means that the robot has a high portability for independent use.

This article is structured as follows. In Section 2, the design concepts of the RSPA and the soft wearable upper limb rehabilitation robot (SWULRR) driven by RSPAs are introduced. In Section 3, the movements of the SWULRR are reported, and the wrist joint is considered as an example in a detailed analysis. In Section 4, the mechanical and kinematic characteristics of the RSPA and SWULRR are studied and evaluated experimentally. Finally, conclusions and future research directions of this study are reported in Section 5.
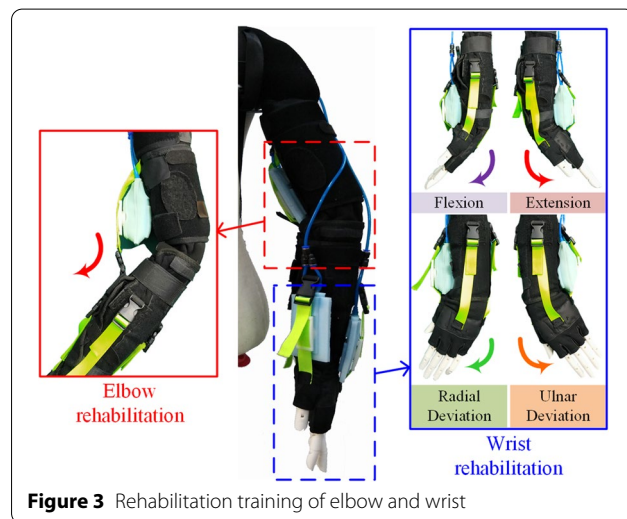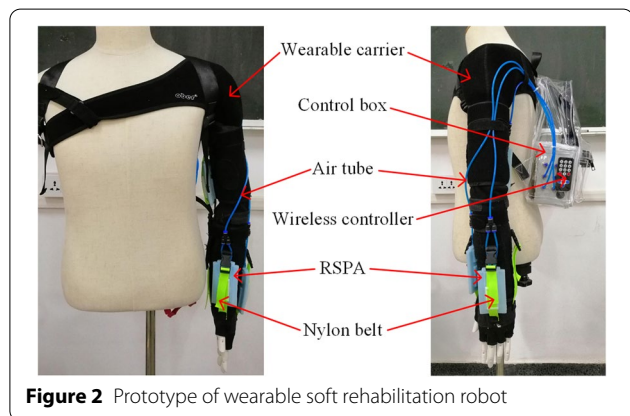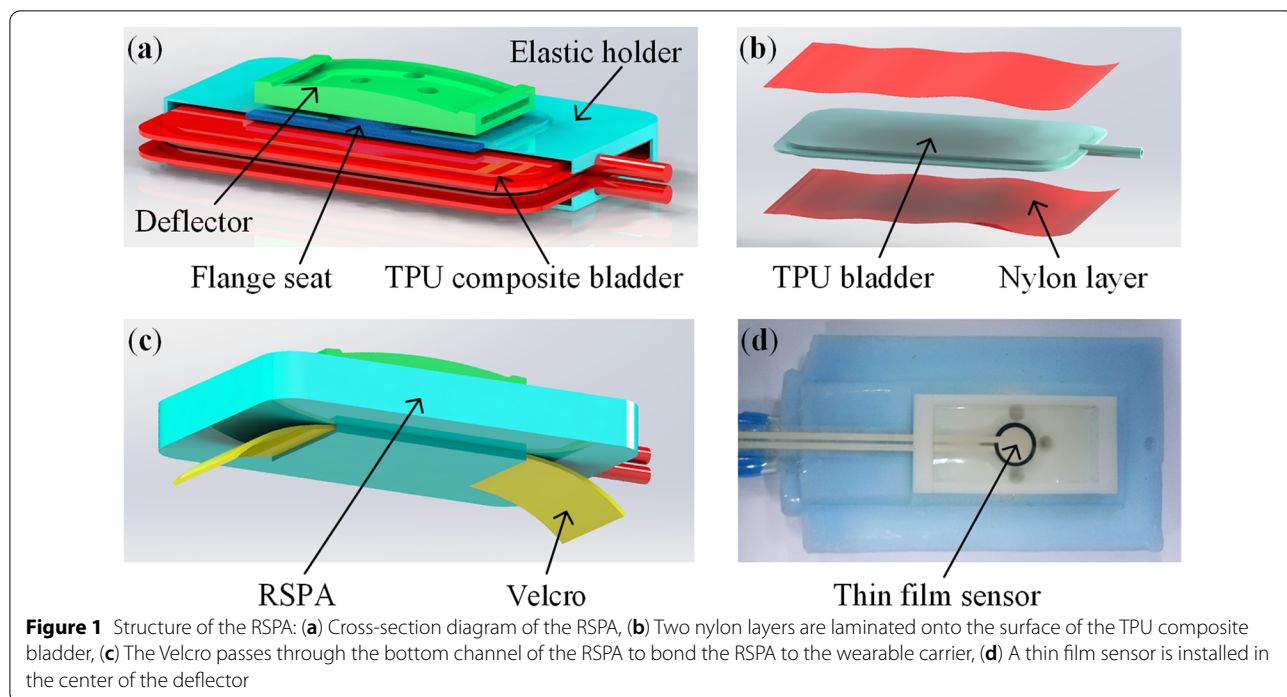
2 Design Concept
2.1 Design of RSPA
As shown in Figure 1(a)–(c), the RSPA is mainly composed of an elastic holder, a flange seat, a deflector and two TPU composite bladders. The flange seat and TPU composite bladders are embedded inside an elastic holder composed of silicone rubber. The TPU composite bladder is mainly composed of a TPU film and laminated with a high-strength fiber material on the surface to form a reinforced bladder structure. The bottom of the flange seat is fixed with a TPU composite bladder and wrapped in an elastic holder. The head of the flange seat extended from the elastic holder and was connected to the deflector using bolts. A rectangular channel was designed in the deflector to facilitate the passage of the nylon belt and to slide it in. Both ends of the nylon belt were connected to a wearable carrier. In addition, a rectangular channel was also reserved at the bottom of the elastic holder, through which the RSPA was attached to the wearable carrier by Velcro. In this way, RSPAs can be installed at the appropriate position of the wrist joint or elbow joint according to the rehabilitation requirements.

As shown in Figure 1(d), there is a thin film sensor at the center of the deflector, which can measure the extrusion pressure between the RSPA and the nylon belt and transmit the pressure signal to the computer to avoid potential secondary damage to the patient caused by excessive force.

2.2 Design of SWULRR
The proposed SWULRR is composed of several modules fixed on a wearable carrier, including the RSPA, control system, and air tube modules, as shown in Figure 2. The wearable carrier consists of five segments: palm, forearm, elbow, upper arm and shoulder, which are designed in accordance with ergonomic standards. The wearable carrier is made of a medical fabric, which is soft, comfortable

Chen *et al. Chinese Journal of Mechanical Engineering*   (2022) 35:83

Page 3 of 9

Figure 1 Structure of the RSPA: (**a**) Cross-section diagram of the RSPA, (**b**) Two nylon layers are laminated onto the surface of the TPU composite bladder, (**c**) The Velcro passes through the bottom channel of the RSPA to bond the RSPA to the wearable carrier, (**d**) A thin film sensor is installed in the center of the deflector

Figure 2 Prototype of wearable soft rehabilitation robot

Figure 3 Rehabilitation training of elbow and wrist

and elastic. The tightness of the wearable carrier can be adjusted according to the needs of the patients to ensure comfort.

The RSPA is fixed onto the wearable carrier through a nylon belt and Velcro, which can be installed at the corresponding position of the wrist joint or elbow joint according to the rehabilitation requirements. When the RSPA acts, the TPU composite bladder inflates and pushes the nylon belt outwards. As the nylon belt cannot be extended, the distance between the connection points of the belt decreases. In this way, the wearable carrier is bent, and the joint is driven to rotate. Taking the wrist joint as an example, and considering only two degrees of freedom of movement of the wrist joint, it is necessary

to arrange four RSPAs around the wrist joint to drive the wrist to perform rehabilitation movements, as shown in Figure 3.

The control system module in the SWULRR is arranged in a control box designed based on the principle of minimum volume, and mainly includes air pumps, control valves, control circuits, and pneumatic pipelines. The control strategy of each joint rehabilitation motion can be realized by a specific default action and force policy, which has the advantages of

Chen *et al. Chinese Journal of Mechanical Engineering*   (2022) 35:83

Page 4 of 9

real-time control and a high-frequency of human-robot interactions. The size of the control box was 250 mm ×150 mm × 100 mm, and its weight was only 2.8 kg. The control box is carried by the user in a backpack, which fully meets the requirements of portability, and eliminates restrictions on the time and place of use. To improve the practicability and intelligence of the SWULRR, the control system is equipped with various force sensors for realizing a multi-control mode, including automatic, manual, and boost modes, which can be switched between using an infrared wireless remote control. In the automatic mode, the rehabilitation robot can perform scientific training according to a preset training plan. In the manual mode, patients can perform independent training according to their needs.

3 Motion Analysis

The function of the SWULRR designed in this work is mainly realized by the inflation and expansion of the TPU composite bladders contained in the RSPA arranged around the wrist or elbow joint, which can drive the corresponding joint to rotate. Because each joint adopts the same RSPA and the motion mechanism is identical, the wrist joint was selected for detailed motion analysis.

As shown in Figure 4, *ABCD* is the initial position of the nylon belt when the TPU composite bladders are not expanded. Point *A* is the fixed position of the nylon belt on the arm, and point *D* is the fixed position of the nylon belt on the hand. Line *AD* is the contact surface between the arm and RSPA, which is parallel to the arm axis. When the TPU composite bladders are inflated, the nylon belt reaches the *A'B'C'D* position.

Applying the Pythagorean theorem on the right triangle $B'A'P_1$, the distance between point A' and point B' can be expressed as follows:

$$l_{A'B'}^2 = [h + \Delta h + L_A - r_A \sin(\alpha + \varphi)]^2 \\ + [L_B + r_A \cos(\alpha + \varphi)]^2, \quad (1)$$

where h is the distance between the deflector and the bottom surface of the RSPA, Δh is the expansion height of the deflector after the TPU composite bladders have been inflated, L_A is the distance between the wrist joint rotation center O and the bottom surface of the RSPA, L_B is the projection length on the arm axis of the distance between point B and point O, r_A is the distance from point A to point O, ϕ is the angle between line AO and the arm axis, and α is the rotation angle of the wrist joint.

The relationship between the rotation angle α of the wrist and the expansion height Δh of the RSPA can be expressed as follows:
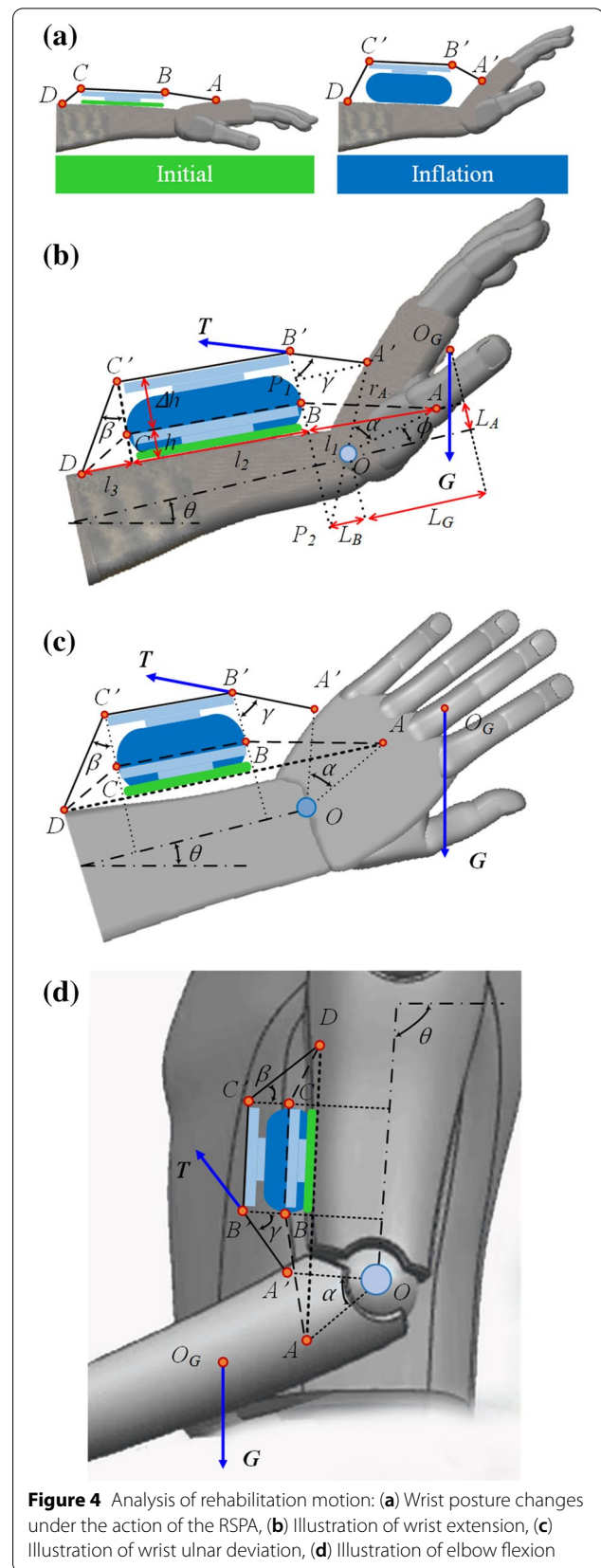

Figure 4 Analysis of rehabilitation motion: (**a**) Wrist posture changes under the action of the RSPA, (**b**) Illustration of wrist extension, (**c**) Illustration of wrist ulnar deviation, (**d**) Illustration of elbow flexion

Chen *et al. Chinese Journal of Mechanical Engineering* (2022) 35:83

Page 5 of 9

$$\alpha = \arcsin\frac{R}{\sqrt{J^2 + K^2}} + \arcsin\frac{K}{\sqrt{J^2 + K^2}} - \varphi, \quad (2)$$

where $J = 2r_A(h + \Delta h + L_A)$, $K = 2L_B r_A$, $R = (h + \Delta h + L_A)^2 + L_B^2 + r_A^2 + l_{A'B'}^2$.

Because the length of the nylon belt is constant, it can be obtained from the following geometric relationship:

$$r_A = \sqrt{L_A^2 + (l_1 + L_B)^2}, \quad (3)$$

$$\begin{aligned} l_{A'B'} &= l_{AB} - (l_{C'D'} - l_{CD}) \\ &= \sqrt{h^2 + l_1^2} - \sqrt{(h + \Delta h)^2 + l_3^2} + \sqrt{h^2 + l_3^2}, \end{aligned} \quad (4)$$

where, l_1, l_2 and l_3 are the projection lengths of lines AB, BC and CD on the bottom surface of the RSPA at the initial time.

The torque-equilibrium equation at the center of the wrist joint can be expressed as follows:

$$\boldsymbol{T} \cdot L_T - \boldsymbol{G} \cdot L_G \cos(\alpha + \theta) = 0, \quad (5)$$

where $\boldsymbol{T}$ is the force of the nylon belt on the hand; L_T is the distance between point O and line AB; $\boldsymbol{G}$ is the gravitation of the hand; L_G is the projection distance between the center of the hand gravity and the joint rotation center O on the arm axis at the initial torque; θ is the angle between the arm axis and the horizontal plane.

The force of the nylon belt can be expressed as follows:

$$\boldsymbol{T} = \frac{\boldsymbol{G} L_G \cos(\alpha + \theta)}{L_T}, \quad (6)$$

L_T can be expressed as follows according to the geometric relationship.

$$L_T = \left(h + \Delta h - \frac{L_B}{\tan\gamma} + L_A\right)\sin\gamma, \quad (7)$$

where, γ is the angle between line $A'B'$ and line BB'.

Lines BB' and $A'O$ are extended and intersect at point P_2. The value of γ can be obtained using the cosine law on triangle $B'P2A'$.

$$\gamma = \arccos\left(\frac{\overline{B'P_2}^2 + \overline{B'A'}^2 - \overline{A'P_2}^2}{2\overline{B'P_2} \cdot \overline{B'A'}}\right), \quad (8)$$

where
$\overline{B'P_2} = h + \Delta h + L_A + L_B \tan(\alpha + \theta)$, $\quad \overline{B'A'} = l_{A'B'}$,
$\overline{A'P_2} = r_A + \frac{L_B}{\cos(\alpha + \varphi)}$.

The expression of the function $T(\Delta h)$ can be obtained by substituting Eqs. (2), (7) and (8) into Eq. (6). When the

RSPA expansion height is Δh, the required force in the direction perpendicular to line BC can be expressed as

$$\boldsymbol{F}_{\mathbf{ac}} = \boldsymbol{T}(\Delta h) \cdot (\cos\beta + \cos\gamma), \quad (9)$$

where $\beta = \arctan\frac{l_3}{h + \Delta h}$, β is the angle between line $B'C'$ and line $C'D'$.

From the above analysis, it can be concluded that the expansion height, RSPA force, and rotation angle of the injured joint are correlated. The input and output parameters of the SWULRR can be solved according to the given parameters.
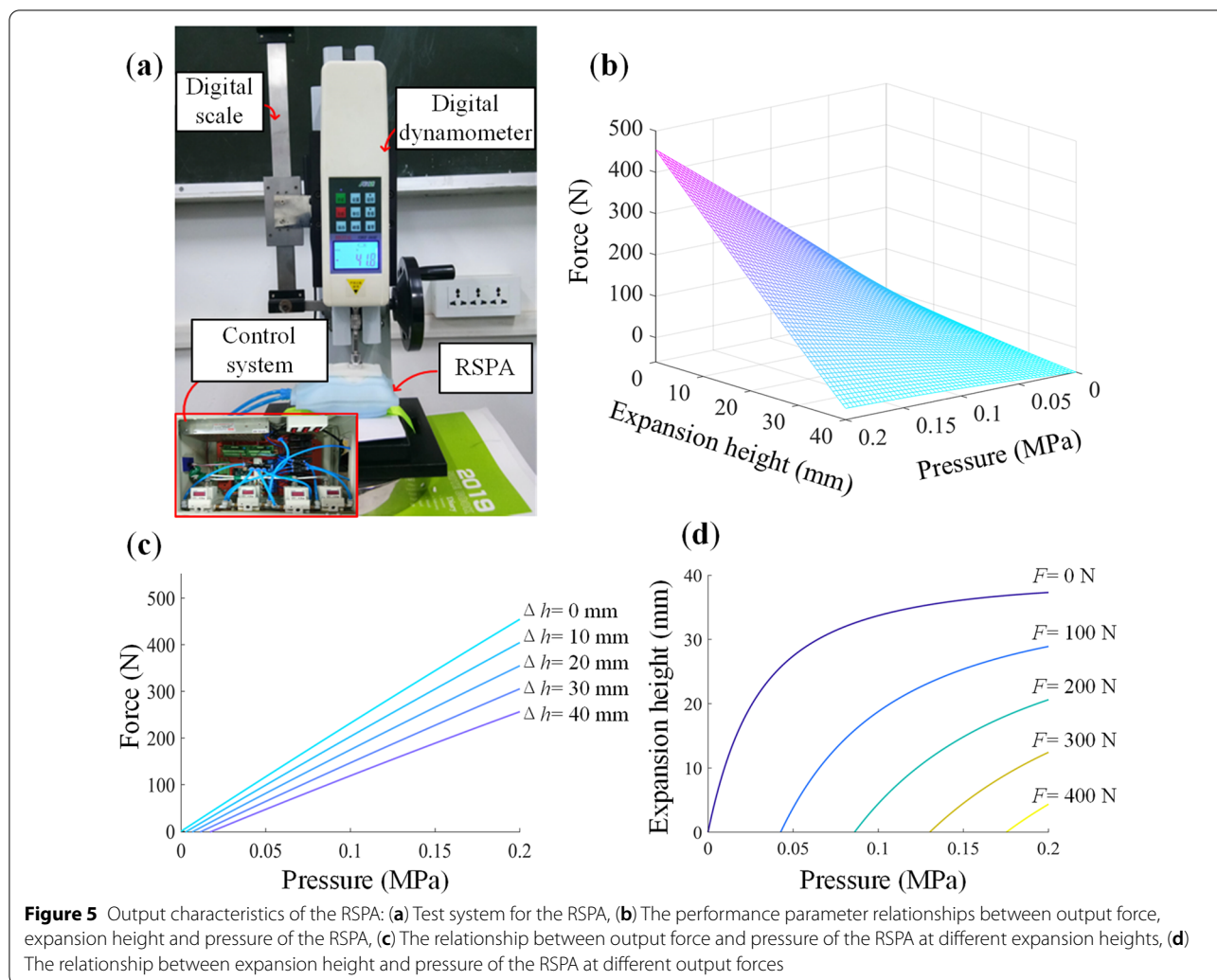
4 Experimental Study

To determine the relationship between the expansion height of the RSPA under the actions of resistance and inflation pressure, a test of the RSPA is carried out based on a force measuring system, which consists of a digital dynamometer, a digital scale, and a control system, as shown in Figure 5(a). Both the digital dynamometer and the digital scale have data storage and communication functions. The data can be transmitted to the host computer, which records the test process and displays the change curve.

In the experiment, different pressures were applied to the TPU composite bladders in the RSPA, and the expansion height of the RSPA was controlled by changing the dynamometer position under a given pressure. The value of the expansion height can be read using a digital scale, and the force on the RSPA can be read using the dynamometer. The relationship between the pressure, force, and expansion height of the RSPA is illustrated in Figure 5(b).

To more intuitively observe the relationship between the three parameters, five curves showing the relationship between the force and the inflation pressure were selected and drawn, as shown in Figure 5(c), for an expansion height of the RSPA of 0, 10, 20, 30 and 40 mm. Then, five curves of the relationship between the expansion height and the inflation pressure were selected and drawn, as shown in Figure 5(d), for a force of 0, 100, 200, 300 and 400 N. It can be observed from Figure 5(c)–(d) that when the expansion heights are identical, an increase in pressure increases the bearing capacity of the RSPA. When the loading forces are identical, an increase in inflation pressure increases the expansion height of the RSPA. When the inflation pressures are identical, an increase in force reduces the expansion height of the RSPA.
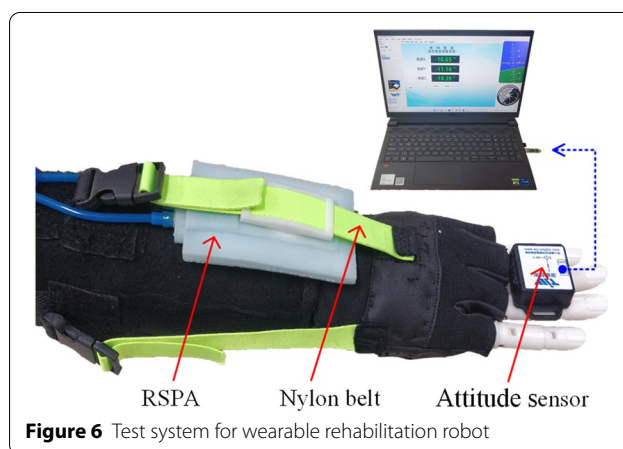
The relationship between the joint rotation angle and the expansion height of the RSPA can be obtained from the abovementioned motion analysis. Therefore, a patient
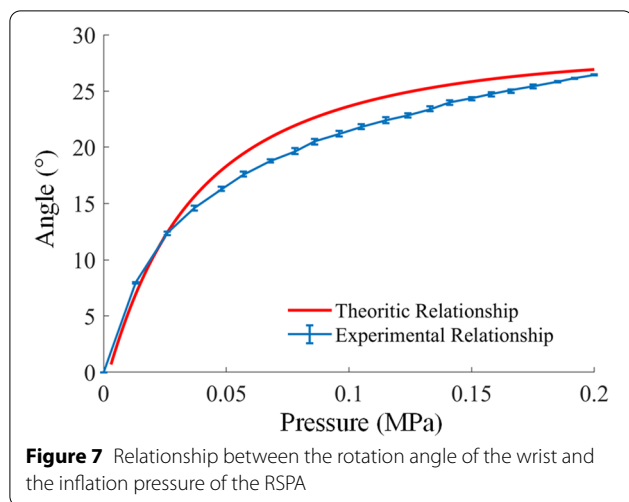
Figure 5 Output characteristics of the RSPA: (**a**) Test system for the RSPA, (**b**) The performance parameter relationships between output force, expansion height and pressure of the RSPA, (**c**) The relationship between output force and pressure of the RSPA at different expansion heights, (**d**) The relationship between expansion height and pressure of the RSPA at different output forces

can determine the appropriate inflation pressure according to the angle of the injured joint and the force required for rehabilitation training.

When RSPAs are used in SWULRR, the rehabilitation training effect must be measured. To eliminate the interference of human factors, an experimental test was conducted with an artificial limb, as shown in Figure 6.

In the experiment, an RSPA installed at the wrist joint was inflated by different air pressures, and the wrist rotation angle data were recorded by the attitude sensor installed on the hand. The angle changes of the wrist joint under the actions of different air pressures were detected by an attitude sensor, and the angle data were sent to the host computer through a Bluetooth module for real-time recording. The relationship curve

Figure 6 Test system for wearable rehabilitation robot

Figure 7 Relationship between the rotation angle of the wrist and the inflation pressure of the RSPA

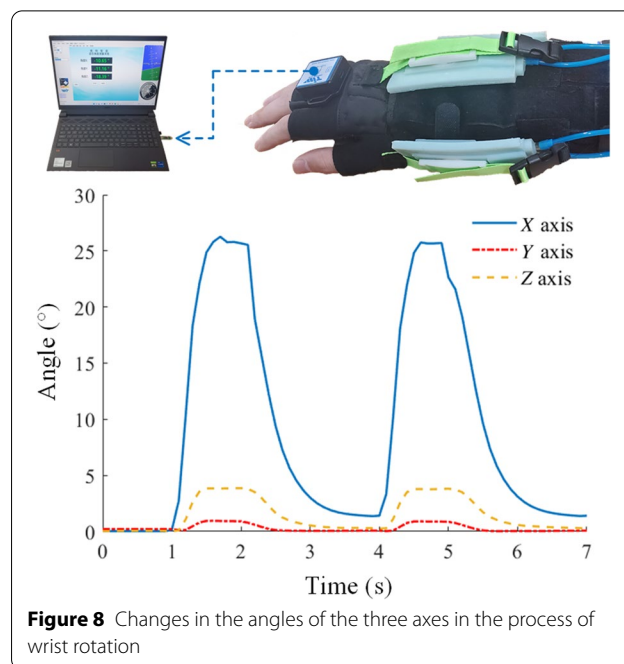**Figure 8** Changes in the angles of the three axes in the process of wrist rotation

between the inflation pressure of the RSPA and the rotation angle of the wrist fitted onto the experimental measurements is marked by a blue line in Figure 7, and the relationship curve between the inflation pressure of the RSPA and the rotation angle of the wrist, which is deduced by motion theory, is marked by a red line in Figure 7.

It can be observed from Figure 7 that there are some errors between the experimental curve and the theoretical curve for a range of the inflation pressure from 0 to 0.2 MPa, and the maximum nominal error is 8.7%. It can be found that the error is mainly due to the damping of the SWULRR in the process of wrist rehabilitation movement. Therefore, at an identical air pressure of the RSPA, the actual rotation angle of the wrist joint was smaller than the theoretical rotation angle.

It can also be observed from Figure 7 that the wrist rotation angle range was 0°–26.4°. According to the analysis above, the rehabilitation training angle of the wrist can be controlled by expanding the RSPA. Therefore, the expansion height of the RSPA can be increased by increasing the number of TPU composite bladders, thereby increasing the rotation angle of the joint. In other words, the number of TPU composite bladders inside the RSPA can be determined based on the training angle required for each joint.

To study the compliance and safety of the SWULRR in practical rehabilitation training, the wrist joint was selected for a joint motion characteristic experiment using RSPAs. The angle data of the wrist joint were obtained using an attitude sensor installed on the hand and sent to the host computer for real-time recording. The recorded angle change curve of the wrist joint is shown in Figure 8.

As shown in Figure 8, the movements of the soft rehabilitation robot are compliant and do not cause a secondary injury to the joint during unidirectional movements of the wrist joint, making it safe.

5 Conclusions and Future Work

Correct and scientific rehabilitation training can help patients quickly recover the function of each effected upper limb joint. Conventional rehabilitation robots mostly adopt a rigid exoskeleton structure, which has the advantage of precise motion control and can satisfy the requirements of rehabilitation. However, a rigid exoskeleton structure has some disadvantages, such as poor flexibility, being uncomfortable, and the possibility of a secondary injury. In addition, conventional rehabilitation systems have a complex structure, high medical cost, and poor portability, and cannot be used for rehabilitation training according to the needs of patients anytime and anywhere.

A new reinforced soft pneumatic actuator (RSPA), which is mainly composed of an elastic holder and two TPU composite bladders, was proposed in this study. The surface of the TPU bladder was laminated with a layer of high-strength nylon material to form a reinforced TPU bladder structure that could withstand higher air pressure while maintaining the flexibility of conventional bladders. The RSPAs were applied in the development of a soft wearable upper limb rehabilitation robot (SWULRR) prototype, which can provide rehabilitation training for human wrist or elbow joints according to the needs of the patients. The SWULRR adopted a soft

Chen *et al. Chinese Journal of Mechanical Engineering*   (2022) 35:83

Page 8 of 9

structure for great human-robot interaction security and adopted a miniaturized control system for a high portability to guarantee independent use.

The movement of the SWULRR was introduced, and the wrist joint was considered as an example for a detailed analysis. The relationships between the expansion height, output force of the RSPA, and rotation angle of the injured joint of the SWULRR were analyzed and obtained. The input and output parameters of the SWULRR can be solved according to the given parameters. An experimental platform was built for the RSPA to analyze the relationships between the force, pressure, and expansion height of the RSPA. It is convenient for patients to be able to determine the appropriate inflation pressure according to the angle of the injured joint and the force required for their rehabilitation training. An experimental study on the wrist rotation angle and pressure of the RSPA was conducted to test the effect of the rehabilitation training and verify the rationality of the motion theory analysis. Finally, the process of wrist rehabilitation training was tested and analyzed, which indicated that the wearable rehabilitation robot would not cause secondary injury to the joints and would improve the safety of rehabilitation training.

Future work will focus on a mechanical analysis of the RSPA and an analysis of the performance parameters of the wearable rehabilitation robot. In addition, owing to the extensive use of flexible connections and soft structures in wearable soft rehabilitation devices, precise control of rehabilitation training is still a subject worthy of further study.

Authors' Information
Xinbo Chen, born in 1993, is currently a Ph.D. candidate at *Parallel Robot and Mechatronic System Laboratory of Hebei Province, Yanshan University, China*. His research interests include man-machine systems and soft robotics.
Shuai Zhang, born in 1994, is currently a Ph.D. candidate at *Parallel Robot and Mechatronic System Laboratory of Hebei Province, Yanshan University, China*.
Kaibin Cao, born in 1993. He received his master's degree in mechanical engineering from *Yanshan University, China*, in 2019.
Chunjie Wei, born in 1996, is currently a Ph.D. candidate at *Parallel Robot and Mechatronic System Laboratory of Hebei Province, Yanshan University, China*.
Wumian Zhao, born in 1995, is currently a Ph.D. candidate at *Parallel Robot and Mechatronic System Laboratory of Hebei Province, Yanshan University, China*.
Jiantao Yao, born in 1980, is currently a professor and Ph.D. candidate supervisor at *Parallel Robot and Mechatronic System Laboratory of Hebei Province* and *Key Laboratory of Advanced Forging & Stamping Technology and Science of Ministry of National Education, Yanshan University, China*. His main research interests include mechatronics, engineering, sensors and soft robotics.

Competing Interests
The authors declare no competing financial interests.

Author Details
[1] Parallel Robot and Mechatronic System Laboratory of Hebei Province, Yanshan University, Qinhuangdao 066004, China. [2] Key Laboratory of Advanced Forging & Stamping Technology and Science of Ministry of National Education, Yanshan University, Qinhuangdao 066004, China.

References
[1] D Shi, W Zhang, W Zhang, et al. A review on lower limb rehabilitation exoskeleton robots. *Chinese Journal of Mechanical Engineering*, 2019, 32(1): 74.
[2] Z Chen, Q Guo, H Xiong, et al. Control and implementation of 2-DOF lower limb exoskeleton experiment platform. *Chinese Journal of Mechanical Engineering*, 2021, 34: 22.
[3] R Gassert, V Dietz. Rehabilitation robots for the treatment of sensorimotor deficits: a neurophysiological perspective. *Journal of Neuroengineering and Rehabilitation*, 2018, 15(1): 46.
[4] G Morone, I Cocchi, S Paolucci, et al. Robot-assisted therapy for arm recovery for stroke patients: state of the art and clinical implication. *Expert Review of Medical Devices*, 2020, 17(3): 223-223.
[5] H Rodgers, H Bosomworth, H I Krebs, et al. Robot assisted training for the upper limb after stroke (RATULS): a multicentre randomised controlled trial. *The Lancet*, 2019, 394(10192): 51–62.
[6] Q Wu, Y Chen. Development of an intention-based adaptive neural cooperative control strategy for upper-limb robotic rehabilitation. *IEEE Robotics and Automation Letters*, 2021, 6(2): 335–342.
[7] E Pirondini, M Coscia, S Marcheschi, et al. Evaluation of the effects of the arm light exoskeleton on movement execution and muscle activities: a pilot study on healthy subjects. *Journal of Neuro Engineering and Rehabilitation*, 2016, 13(1): 9.
[8] U Keller, H J A van Hedel, V Klamroth-Marganska, et al. ChARMin: the first actuated exoskeleton robot for pediatric arm rehabilitation. *IEEE/ASME Transactions on Mechatronics*, 2016, 21(5): 2201–2213.
[9] Q Wu, X Wang, B Chen, et al. Development of a minimal-intervention-based admittance control strategy for upper extremity rehabilitation exoskeleton. *IEEE Transactions on Systems, Man, and Cybernetics: Systems*, 2018, 48(6): 1005–1016.
[10] Z Li, H Xie, W Li, et al. Proceeding of human exoskeleton technology and discussions on future research. *Chinese Journal of Mechanical Engineering*, 2014, 27(3): 437–447.
[11] R A R C Gopura, D S V Bandara, K Kiguchi, et al. Developments in hardware systems of active upper-limb exoskeleton robots: A review. *Robotics and Autonomous Systems*, 2016, 75: 203–220.
[12] E Akdoğan, M E Aktan, A T Koru, et al. Hybrid impedance control of a robot manipulator for wrist and forearm rehabilitation: Performance analysis and clinical results. *Mechatronics*, 2018, 49: 77–91.
[13] B Brahmi, M Saad, C Ochoa-Luna, et al. Adaptive tracking control of an exoskeleton robot with uncertain dynamics based on estimated time-delay control. *IEEE/ASME Transactions on Mechatronics*, 2018, 23(2): 575–585.

[14] J D Sanjuan, A D Castillo, M A Padilla, et al. Cable driven exoskeleton for upper-limb rehabilitation: A design review. *Robotics and Autonomous Systems*, 2020, 126: 103445.

[15] J Sung, S Choi, H Kim, et al. Feasibility of rehabilitation training with a newly developed, portable, gait assistive robot for balance function in hemiplegic patients. *Annals of Rehabilitation Medicine*, 2017, 41(2): 178.

[16] Q Wu, X Wang, B Chen, et al. Development of an RBFN-based neural-fuzzy adaptive control strategy for an upper limb rehabilitation exoskeleton. *Mechatronics*, 2018, 53: 85–94.

[17] K Xu, J Zhao, D Qiu, et al. A pilot study of a continuum shoulder exoskeleton for anatomy adaptive assistances. *Journal of Mechanisms and Robotics*, 2014, 6(4): 041011.

[18] A Alamdari, V Krovi. Design and analysis of a cable-driven articulated rehabilitation system for gait training. *Journal of Mechanisms and Robotics*, 2016, 8(5): 051018.

[19] X Cui, W Chen, X Jin, et al. Design of a 7-DOF cable-driven arm exoskeleton (CAREX-7) and a controller for dexterous motion training or assistance. *IEEE/ASME Transactions on Mechatronics*, 2017, 22(1): 161–172.

[20] Y Wang, Q Xu. Design and testing of a soft parallel robot based on pneumatic artificial muscles for wrist rehabilitation. *Scientific Reports*, 2021, 11(1): 1273.

[21] J Wang, Y Fei, W Chen. Integration, sensing, and control of a modular soft-rigid pneumatic lower limb exoskeleton. *Soft Robotics*, 2020, 7(2): 140–154.

[22] Q Liu, J Zuo, C Zhu, et al. Design and control of soft rehabilitation robots actuated by pneumatic muscles: State of the art. *Future Generation Computer Systems*, 2020, 113: 620–634.

[23] J Jeong, I B Yasir, J Han, et al. Design of shape memory alloy-based soft wearable robot for assisting wrist motion. *Applied Sciences*, 2019, 9(19): 4025.

[24] L Toth, A Schiffer, M Nyitrai, et al. Developing an anti-spastic orthosis for daily home-use of stroke patients using smart memory alloys and 3D printing technologies. *Materials & Design*, 2020, 195: 109029.

[25] J Fang, J Yuan, M Wang, et al. Novel accordion-inspired foldable pneumatic actuators for knee assistive devices. *Soft Robotics,* 2020, 7(1): 95–108.

[26] A J Veale, K Staman, H van der Kooij, et al. Soft, wearable, and pleated pneumatic interference actuator provides knee extension torque for sit-to-stand. *Soft Robotics*, 2021, 8(1): 28–43.

[27] D Cafolla, M Russo, G. Carbone. CUBE, a cable-driven device for limb rehabilitation. *Journal of Bionic Engineering*, 2019, 16(3): 492–502.

[28] M Laribi, G Carbone, S Zeghloul. On the optimal design of cable driven parallel robot with a prescribed workspace for upper limb rehabilitation tasks. *Journal of Bionic Engineering*, 2019, 16(3): 503–513.

[29] N Li, T Yang, P Yu, et al. Bio-inspired upper limb soft exoskeleton to reduce stroke-induced complications. *Bioinspiration & Biomimetics*, 2018, 13(6): 066001.

[30] G Andrikopoulos, G Nikolakopoulos, S Manesis. Design and development of an exoskeletal wrist prototype via pneumatic artificial muscles. *Meccanica*, 2015, 50(11): 2709–2730.

[31] V W Oguntosin, Y Mori, H Kim, et al. Design and validation of exoskeleton actuated by soft modules toward neurorehabilitation—vision-based control for precise reaching motion of upper limb. *Frontiers in Neuroscience*, 2017, 11: 352.

[32] C T O'Neill, C M McCann, C J Hohimer, et al. Unfolding textile-based pneumatic actuators for wearable applications. *Soft Robotics*, 2021, 9(1):163-172.

[33] A Vidal, J Morales, G Ortiz-Torres, et al. Soft exoskeletons: Development, requirements, and challenges of the last decade. *Actuators*, 2021, 10(7): 166.

[34] X Li, Y Pan, G Chen, et al. Adaptive human–robot interaction control for robots driven by series elastic actuators. *IEEE Transactions on Robotics*, 2017, 33(1): 169–182.

[35] S Lessard, P Pansodtee, A Robbins, et al. A soft exosuit for flexible upper-extremity rehabilitation. *IEEE Transactions on Neural Systems and Rehabilitation Engineering*, 2018, 26(8): 1604–1617.

[36] C Nam, W Rong, W Li, et al. An exoneuromusculoskeleton for self-help upper limb rehabilitation after stroke. *Soft Robotics*, 2020, 9(1): 14-35.